The Journal of Chemical Physics

Ab initio spectroscopic characterization of the radical CH_3OCH_2 at low temperatures

Cite as: J. Chem. Phys. **150**, 194102 (2019); https://doi.org/10.1063/1.5095857
Submitted: 13 March 2019 . Accepted: 24 April 2019 . Published Online: 15 May 2019

O. Yazidi, M. L. Senent, V. Gámez, M. Carvajal, and M. Mogren Al-Mogren

The Journal of Chemical Physics ARTICLE scitation.org/journal/jcp

Ab initio spectroscopic characterization of the radical CH_3OCH_2 at low temperatures

Cite as: J. Chem. Phys. 150, 194102 (2019); doi: 10.1063/1.5095857
Submitted: 13 March 2019 • Accepted: 24 April 2019 •
Published Online: 15 May 2019

O. Yazidi,[1] M. L. Senent,[2,a)] V. Gámez,[2] M. Carvajal,[3] and M. Mogren Al-Mogren[4]

AFFILIATIONS

[1] Laboratoire de Spectroscopie Atomique Moléculaire et Applications, Faculté des Sciences de Tunis, Université de Tunis El Manar, Tunis 2092, Tunisia
[2] Departamento de Química y Física Teóricas, Instituto de Estructura de la Materia, IEM-CSIC, Serrano 121, Madrid 28006, Spain and Unidad Asociada GIFMAN, CSIC-UHU, 21071 Huelva, Spain
[3] Dpto. Ciencias Integradas, Centro de Estudios Avanzados en Física, Matemática y Computación, Facultad de Ciencias Experimentales, Universidad de Huelva, Unidad Asociada GIFMAN, CSIC-UHU, 21071 Huelva, Spain and Instituto Universitario Carlos I de Física Teórica y Computacional, Universidad de Granada, Granada, Spain
[4] Chemistry Department, Faculty of Science, King Saud University, P.O. Box 2455, Riyadh 11451, Kingdom of Saudi Arabia

[a)] **Author to whom correspondence should be addressed:** ml.senent@csic.es

ABSTRACT

Spectroscopic and structural properties of methoxymethyl radical (CH_3OCH_2, RDME) are determined using explicitly correlated *ab initio* methods. This radical of astrophysical and atmospheric relevance has not been fully characterized at low temperatures, which has delayed astrophysical research. We provide rovibrational parameters, excitations to the low energy electronic states, torsional and inversion barriers, and low vibrational energy levels. In the electronic ground state (X^2A), which appears "clean" from nonadiabatic effects, the minimum energy structure is an asymmetric geometry whose rotational constants and dipole moment have been determined to be A_0 = 46 718.67 MHz, B_0 = 10 748.42 MHz, and C_0 = 9272.51 MHz, and 1.432D (μ_A = 0.695D, μ_B = 1.215D, μ_C = 0.302D), respectively. A variational procedure has been applied to determine torsion-inversion energy levels. Each level splits into 3 subcomponents (A_1/A_2 and E) corresponding to the three methyl torsion minima. Although the potential energy surface presents 12 minima, at low temperatures, the infrared band shapes correspond to a surface with only three minima because the top of the inversion V^{α} barrier at $\alpha = 0^{\circ}$ (109 cm^{-1}) stands below the zero point vibrational energy and the CH_2 torsional barrier is relatively high (~2000 cm^{-1}). The methyl torsion barrier was computed to be ~500 cm^{-1} and produces a splitting of 0.01 cm^{-1} of the ground vibrational state.

INTRODUCTION

Radicals play important roles in atmospheric and in interstellar chemistry. In gas-phase sources and grains of the interstellar medium, they can induce exothermic and no activation energy processes.[1–3] In the atmosphere, most of the chemical reactions involve reactive free radicals that are generated by photochemical processes from stable precursors. Methoxymethyl radical (CH_3OCH_2, RDME) is produced as a result of removing one methyl hydrogen from dimethyl ether (CH_3OCH_3, DME). Atmospheric degradation of DME can be initiated via hydrogen subtraction by OH radicals, molecular oxygen, or atomic hydrogen to produce RDME.[4–6] Experimental and theoretical studies aiming to clarify the mechanisms of DME oxidation in the atmosphere are recurrent.[7–18] Since DME is an abundant interstellar molecule, H subtraction processes have been studied at very low temperatures obtaining RDME as a product.[1]

The application of dimethyl ether as an alternative fuel has motivated frequent previous kinetic studies where RDME appears as a common product.[8] However, spectroscopic studies are quite limited. The UV absorption spectrum of the CH_3OCH_2 radical was recorded by Langer *et al.*[19] in the gas phase. The pulse radiolysis of a mixture containing DME led to a rapid increase in the UV absorption at 230 nm associated with RDME. Broad bands were observed

between 3.5 and 5.6 eV (1 eV = 1.602 176 × 10^{-19} J).[19] Vertical excitation energies computed using multireference configuration interaction theory (MRCI) and a double zeta basis set[20] allowed one to identify the excitation to the first excited electronic state with the band observed at 4.13 eV.[19] Four states with doublet spin-multiplicity character were predicted at 4.03, 5.16, 6.83, and 7.44 eV.[20]

To date, there are no available measurements of the rotational spectra of the methoxymethyl radical. In fact, to our knowledge, there is only a unique published paper addressing the infrared (IR) spectrum.[21] Recently, Gong and Andrews have recorded the IR spectrum in the Ar matrix[21] characterizing four infrared absorptions at 1468.1, 1253.9, 1226.6, and 944.4 cm^{-1}, which were assigned by deuterium substitution as well as by frequency and intensity calculations using density functional theory.

In astrophysical models, RDME is considered a possible intermediate of processes connecting the two abundant species DME and methyl formate[3] and it is considered a detectable species. The discovery of new molecules requires a previous laboratory characterization that, in our case, involves intricate experiments due to the high reactivity of radicals. The lack of available spectroscopic parameters and the enormous astrophysical interest are the motivation of the present paper which aims to obtain as much as possible information that can be derived from state-of-the-art *ab initio* calculations. We search to determine accurate theoretical parameters for further spectral assignments and further astrophysical searches. Highly correlated *ab initio* methods are employed to obtain reliable rovibrational parameters (rotational constants, centrifugal distortion constants, vibrational band centers, etc.), the dipole moment, excitation to the low excited electronic states, and an exhaustive description of the far infrared spectral region.

RDME can be defined as nonrigid species because the ground electronic state potential energy surface (PES) presents 12 minima connected by large amplitude motions. Three internal large amplitude modes are responsible for the nonrigidity: the methyl group and the CH_2 group torsions and the CH_2 inversion. Because the methyl torsion barrier and the inversion barrier are much lower than the CH_2 torsional barrier, in principle, the low energy levels can be calculated using a variational two-dimensional model. This allows us to obtain splittings of the levels due to the tunneling effect.

COMPUTATIONAL DETAILS

The equilibrium structure and the two-dimensional potential energy surface of RDME were calculated with explicitly correlated coupled cluster theory, RCCSD(T)-F12b,[22,23] implemented in MOLPRO[24] using the corresponding default options. Furthermore, a full-dimensional anharmonic force field was computed with second order Möller-Plesset theory (MP2) implemented in GAUSSIAN.[25] This force field was applied to determine the vibrational corrections of the surface and the anharmonic contributions[26] which are less dependent on the level of theory than the first order spectroscopic properties. The aug-cc-pVTZ basis set (denoted by AVTZ)[27] was used in the MP2 calculations. For the RCCSD(T)-F12 calculations, the AVTZ atomic orbitals were employed in connection with the corresponding basis sets for the density fitting and the resolution of the identity.

Vertical excitation energies to the excited electronic states were determined with the complete active space self-consistent field (CASSCF) method[28,29] followed by the internally contracted multireference configuration interaction approach (MRCI).[30,31] Both methods are implemented in MOLPRO.[24]

For the two modes responsible for the nonrigidity being the methyl torsion and the CH_2 wagging (or inversion) modes, the energies were calculated using the original program ENEDIM[32] and a variational model of reduced dimensionality. More details concerning the theory implemented in ENEDIM theory, as well as examples of previous applications, can be found in Refs. 33–38.

RESULTS AND DISCUSSION

Electronic ground state: Molecular structure and rotational parameters

The most stable structure of RDME shown in Fig. 1 is an asymmetric geometry that can be classified in the C_1 point group. Three large amplitude motions, the CH_3 and the CH_2 internal rotations, and the CH_2 wagging, intertransform the 12 minima of the electronic ground state potential energy surface. Since the splitting of the CH_2 torsion is not going to have any effect in the calculations of the present work given the height of the corresponding barrier, the far infrared spectrum can be explored using a two-dimensional model and the levels can be classified using the molecular symmetry group G_6.[39,40] Thus, in this paper, the CH_3 torsion and the CH_2 wagging are treated as large amplitude vibrations responsible for the minimum intertransformation, whereas the CH_2 torsional motion is described by small displacements around the equilibrium position (CH_2 twist). Two symbols θ and α identify the corresponding large amplitude coordinates. α represents the dihedral angle between the C3O1C2 and H7C2H8 planes, whereas the methyl torsional coordinate is defined using three dihedral angles

$$\theta = (\mathrm{H4C3O1C2} + \mathrm{H5C3O1C2} + \mathrm{H6C3O1C2})/3. \quad (1)$$

At the nonplanar equilibrium structure, $\theta^{MIN} = 177.1°$ and $\alpha^{MIN} = 25°$.

Table I collects the structural parameters and the equilibrium rotational constants computed at the RCCSD(T)-F12 level of theory. The dipole moment components were obtained using MP2 calculations.

Table I shows the ground vibrational state rotational parameters corresponding to the Watson S-reduction Hamiltonian (I^r representation).[41] The centrifugal distortion constants were computed

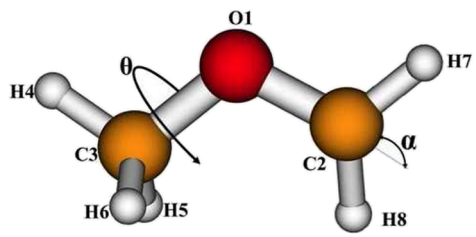

FIG. 1. The minimum energy geometry of RDME. Independent coordinates and atom labeling.

TABLE I. RCCSD(T)-F12b/AVTZ structural and rotational constants. MP2/AVTZ centrifugal distortion constants and dipole moment of the minimum energy geometry of CH_3OCH_2.

Structural parameters (Å, deg)[a]			
O1C2	1.3535	H5C3O1	110.4
O1C3	1.4192	H6C3C1	110.4
H4C3	1.0866	H7C2O1	114.0
H5C3	1.0936	H8C2O1	118.2
H6C3	1.0924	H4C3O1C2	−177.0
H7C2	1.0782	H5C3O1C2	−57.7
H8C2	1.0838	H6C3O1C2	63.5
C2O1C3	115.4	H7C2O1C3	176.9
H4C3O1	107.0	α^{MIN}	25.0
Rotational constants (MHz)			
A_e	46 625.72	A_0	46 718.67
B_e	10 859.71	B_0	10 748.42
C_e	9 367.67	C_0	9 272.51
Centrifugal distortion constants (S reduction, I^r representation)			
Δ_J (MHz)	0.0103	H_J (Hz)	0.0008
Δ_{JK} (MHz)	−0.0357	H_K (Hz)	27.7329
Δ_K(MHz)	0.5832	H_{JK} (Hz)	−1.0954
d_1 (MHz)	−0.0021	H_{KJ} (Hz)	−5.8508
d_2 (MHz)	0.0002	h_1 (Hz)	0.0041
		h_2 (Hz)	0.0029
		h_3 (Hz)	0.0007

Dipole moment (D)[a]

μ	1.432	μ_A	0.695	μ_B	1.215	μ_C	0.302

[a]1 Å = 10^{-10} m; 1D = 3.33564 × 10^{-30} C m.

from an anharmonic MP2 force field. The ground vibrational state rotational constants A_0, B_0, and C_0 were estimated from the corresponding RCCSD(T)-F12 equilibrium parameters (A_e, B_e, and C_e), using the following equation:[36,42–44]

$$B_0 = B_e(\mathrm{RCCSD(T)-F12}) + \Delta B_e^{\mathrm{core}}(\mathrm{RCCSD(T)}) + \Delta B^{\mathrm{vib}}(\mathrm{MP2}), \quad (2)$$

where ΔB^{vib} represents the vibrational contribution to the rotational constants derived from the Vibrational Second Order Perturbation Theory (VPT2), α_r^i represents vibration-rotation interaction parameters determined with the MP2 cubic force field,[45] and ΔB_e^{core} contains the effect of the core-electron correlation.

Although we have not found any available experimental data to assess the present computed rotational parameters, we can expect divergences lower than 10 MHz with the real values. This threshold is sustained by former results obtained for diverse molecular species. Examples are those described in Refs. 36, 42–44. Some of these previous studies, such as the study of 4-hydroxy-2-butynenitrile[42] and dimethylsulfoxide,[44] were performed in collaboration with rotational spectroscopy laboratories. Based on previous studies, we can assert that the predicted rotational constants A_0 = 46 718.67 MHz, B_0 = 10 748.42 MHz, and C_0 = 9272.51 MHz are accurate enough for being employed in further spectrum assignments.

Excited electronic states

Vertical excitation energies to the low excited electronic states were computed at the MRCI/AVTZ level of theory to explore the density of states in the ground state region and to evaluate the risk of vibronic effects due to the radical character of RDME. The resulting energy levels are shown in Fig. 2 where they are classified using the irreducible representations of group C_1 of the minimum energy geometry ($\alpha = \alpha^{MIN}$) and the group C_s of the planar structure corresponding to the top of the CH_2 wagging barrier ($\alpha = 0°$). Both structures are very close in energy (~100 cm^{-1}). The ground electronic state appears "clean" from nonadiabatic effects.

Configuration Interaction (CI) calculations were performed over an active space of 10 orbitals, larger than the 7 orbital space employed in Ref. 20. Nine orbitals were optimized and considered double occupied in all the configurations. The first four electronic states show doublet spin multiplicity, whereas the first quartet state appears over 8 eV.

The X^2A ground electronic state, as well as the low energy excited states, presents a doublet spin-multiplicity character. The first excited state (A^2A) appears at 3.95 eV in a region where a UV broad band has been observed (4.03 eV[19]). This excitation energy is in good agreement with previous calculations (4.13 eV[20]). High density of states characterizes the 3.9–4.7 eV region, as has been experimentally observed.[19]

Infrared spectrum

The fundamental transitions of Table II were estimated using the following formula:

$$E = \sum_i \omega_i^{\mathrm{RCCSD(T)-F12}}\left(v_i + \frac{1}{2}\right) + \sum_{i\geq j} x_{ij}^{MP2}\left(v_i + \frac{1}{2}\right)\left(v_j + \frac{1}{2}\right), \quad (3)$$

where the very accurate theoretical procedure RCCSD(T)-F12 is employed to compute the harmonic contributions ω_i of the vibrational energies, whereas the x_{ij} anharmonic constants are computed from an MP2 full-dimensional anharmonic force field and vibrational second order perturbation theory. v_i and v_j represent the vibrational quanta. VPT2 anharmonic constants x_{ij} are supplied as the supplementary material.

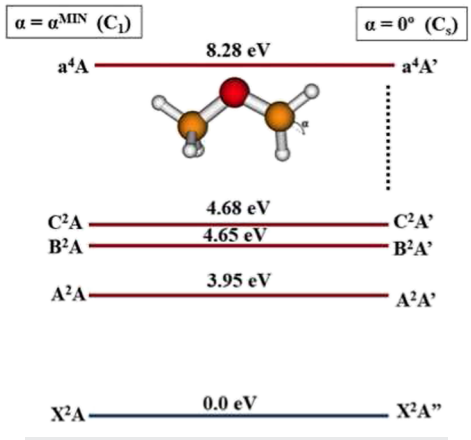

FIG. 2. First four doublet electronic states of RDME.

TABLE II. Vibrational fundamentals (in cm^{-1}) computed using second order perturbation theory (VPT2).

Mode	ω (RCCSD(T)-F12/AVTZ)	ν[a]	Expt.[b]	Assignment
ν_1	3277.9	3160.3		CH_2 asym str
ν_2	3153.7	3016.7		CH_3 asym str
ν_3	3125.7	3031.5		CH_2 sym str
ν_4	3087.2	**2974.3**		CH_3 asym str
ν_5	3018.7	**3013.8**		CH_3 sym str
ν_6	1511.7	1467.7	1468.1	CH_3 def
ν_7	1502.4	**1482.1**		CH_3 def + CH_2 bend
ν_8	1498.2	**1475.1**		CH_3 def
ν_9	1462.2	1429.7		CH_3 def + CH_2 bend
ν_{10}	1295.3	**1258.4**	1253.9	O–CH_2 str
ν_{11}	1262.1	1231.6	1226.6	HCO(CH_2)bend
ν_{12}	1179.2	1153.2		HCO(CH_3)bend
ν_{13}	1141.3	1119.2		HCO(CH_3) bend
ν_{14}	978.9	955.0	944.4	O–CH_3 str
ν_{15}	571.9	**190.9**		CH_2 wag
ν_{16}	437.4	**433.8**		COC bend
ν_{17}	298.5	**241.0**		CH_2 twist
ν_{18}	165.7	146.7		CH_3 torsion

[a]Estimated using Eq. (3); levels displaced by Fermi resonances are emphasized in boldface.
[b]Observed argon matrix infrared wavenumbers.[21]

In principle, within the VPT2 description, all the vibrational modes of RDME are infrared active due to the asymmetric character of the minimum energy geometry.

In Table II, the computed transitions are compared with existing experimental data even though the available material is very limited due to the RDME radical character and high reactivity. One of the few existing papers on spectroscopy was authored by Gong and Andrews[21] who measured the infrared spectrum in solid argon. The spectrum is characterized by four infrared absorptions at 1468.1, 1253.9, 1226.6, and 944.4 cm^{-1}, which were assigned by deuterium substitution and density functional theory. Their values recorded in the Ar matrix are in good agreement with our computed wavenumbers predicted for an isolated molecule.

VPT2 neglects the minimum interconversion effects. For the large amplitude motions responsible for the nonrigidity, a specific theory must be employed as described in the section titled Torsion-wagging 2D-model. However, if the anharmonic force field is accurate enough, usually the VPT2 algorithms implemented in Gaussian allow us to predict the effect of resonances providing valuable initial sets of parameters.[26] Predicted Fermi displacements and the Fermi resonance parameters are supplied as the supplementary material. Within the VPT2 approximation and after considering the Fermi displacements, four vibrational fundamentals are found to lie below 500 cm^{-1}: ν_{15}, ν_{16}, ν_{17}, and ν_{18}. They can be assigned to the CH_2 wagging, COC bending, CH_2 twist, and the methyl torsion, respectively.

Excited VPT2 vibrational energy levels up to 620 cm^{-1} are shown in Table IV. The comparison between the computed and the few experimental data validates the VPT2 theory which fails when high excitation energies of the ν_{15} CH_2 wagging mode are computed. For this mode, anharmonic effects are really overestimated generating too large contributions (i.e., ω_{15} = 571.9 cm^{-1} and ν_{15} = 190.9 cm^{-1}), and in addition, the computed anharmonic overtone is truly inconsistent ($2\omega_{15}$ = 1143.8 cm^{-1} and $2\nu_{15}$ = −20 cm^{-1}). The anharmonic force field components corresponding to ν_{15} are not well established due to the shape of potential energy surface in the double minimum region.

For the large amplitude motions, Fermi displacements are expected to be very small. This fact validates the two-dimensional model described in the section titled Torsion-wagging 2D-model. At the MP2/AVTZ level of theory, the ν_{15} fundamental appears slightly displaced (~−2 cm^{-1}), caused by the resonance between the wagging fundamental and the CH_2 twist overtone. To evaluate these results, it has to be considered that VPT2 fails when spectroscopic parameters involving wagging mode excitations are computed.

Torsion-wagging 2D-model

On the basis of the vibrational energies and the results of the test of Fermi interactions, the CH_3 torsional motion and the CH_2 wagging can be separated from the remaining vibrational modes. Then, to determine variationally the low energies, the following Hamiltonian can be applied:

$$\hat{H}(\theta,\alpha) = -\sum_{i=1}^{2}\sum_{j=1}^{2}\left(\frac{\partial}{\partial q_i}\right)B_{ij}(\theta,\alpha)\left(\frac{\partial}{\partial q_j}\right) + V^{eff}(\theta,\alpha), \quad q_i, q_j = \theta, \alpha. \tag{4}$$

In this equation, $V^{eff}(\theta, \alpha)$ represents the effective potential given by

$$V^{eff}(\theta,\alpha) = V(\theta,\alpha) + V'(\theta,\alpha) + V^{ZPVE}(\theta,\alpha), \tag{5}$$

TABLE III. RCCSD(T)-F12 coefficients (in cm^{-1}) of the effective potential energy surface $V^{eff}(\theta, \alpha)$ according to the symmetry adapted Fourier series [Eq. (6)].

Terms		Coefficient	Terms		Coefficient
A^{00}	1	4493.072	A_{cc}^{61}	cos 3θ cos 6α	−4.026
A_{cc}^{10}	cos α	−3320.696	A_{cc}^{02}	cos 6θ	−0.775
A_{cc}^{20}	cos 2α	−2367.847	A_{cc}^{12}	cos 6θ cos α	0.468
A_{cc}^{30}	cos 3α	522.884	A_{cc}^{22}	cos 6θ cos 2α	0.204
A_{cc}^{40}	cos 4α	2013.802	A_{cc}^{32}	cos 6θ cos 3α	0.773
A_{cc}^{50}	cos 5α	−1280.869	A_{cc}^{42}	cos 6θ cos 4α	1.380
A_{cc}^{60}	cos 6α	284.964	A_{cc}^{52}	cos 6θ cos 5α	−1.106
A_{cc}^{01}	cos 3θ	219.310	A_{cc}^{62}	cos 6θ cos 6α	0.720
A_{cc}^{11}	cos 3θ cos α	21.732	A_{ss}^{11}	sin 3θ sin α	−111.993
A_{cc}^{21}	cos 3θ cos 2α	16.904	A_{ss}^{21}	sin 3θ sin 2α	31.900
A_{cc}^{31}	cos 3θ cos 3α	1.445	A_{ss}^{31}	sin 3θ sin 3α	−13.787
A_{cc}^{41}	cos 3θ cos 4α	−9.024	A_{ss}^{41}	sin 3θ sin 4α	20.143
A_{cc}^{51}	cos 3θ cos 5α	8.576	A_{ss}^{51}	sin 3θ sin 5α	−13.717

where V(θ, α) is the *ab initio* two-dimensional potential energy surface (2D-PES) determined from the total electronic energies of a set of selected geometries. For this purpose, a total number of 32 geometries were chosen for eight different values of the α coordinate (0°, 15°, 30°, 45°, 60°, 75°, 130°, 160°) and four values of the H4C3O1C2 dihedral angle (180°, 90°, −90°, 0°). The two additional conformations with α = 130°,160° were considered to assure a correct fit, although only the six first values of α are needed to describe the shape of surface in the low energy region. In order to take into consideration the neglected vibrational modes, 16 curvilinear internal coordinates were allowed to be relaxed in all the geometries.

The Podolsky pseudopotential V′(θ, α) and the $B_{ij}(\theta, \alpha)$ kinetic energy parameters were determined from the chosen geometries using the ENEDIM code[32] (see Refs. 33 and 34 for details). $V^{ZPVE}(\theta, \alpha)$ represents the zero point vibrational energy correction, which was

TABLE IV. Low vibrational energy levels of CH_3OCH_2 (cm^{-1}).

n_θ, n_α	Sym.	E_{VAR}	VPT2		n_θ, n_α	Sym.	E_{VAR}	VPT2	
0 0	A_1	0.000[a]		0.0	0 2	A_1	507.547	$2\nu_{15}$	
	E	0.010				E	557.318		
1 0	A_2	168.376	ν_{18}	146.7	2 1	A_2	636.522	$2\nu_{18}\nu_{15}$	446.8
	E	168.013				E	636.730		
			ν_{17}	241.0				$2\nu_{17}$	482.2
2 0	A_1	311.708	$2\nu_{18}$	290.6	4 0	A_1	752.051	$4\nu_{18}$	525.4
	E	316.690				E	659.253		
0 1	A_2	328.557	ν_{15}	190.9				$3\nu_{18}\nu_{15}$	559.3
	E	328.505							
			$\nu_{18}\ \nu_{17}$	378.6				$2\nu_{17}\nu_{15}$	564.9
3 0	A_2	456.258	$3\nu_{18}$	409.4				$\nu_{18}\ \nu_{16}$	582.0
	E	423.360							
			ν_{16}	433.8				$2\nu_{17}\nu_{18}$	601.6
1 1	A_1	486.958	$\nu_{18}\ \nu_{15}$	323.9				$3\nu_{18}\nu_{17}$	616.8
	E	496.275							
			$\nu_{17}\ \nu_{15}$	385.2				$\nu_{18}\nu_{15}$	619.6

Kinetic energy parameters and effective potential energy barriers (cm^{-1})

$A^{00}(B_{\theta\theta})$	7.1432	$V_3\ (\alpha = \alpha^{MIN})$	502
$A^{00}(B_{\alpha\alpha})$	32.0043	$V_3\ (\alpha = 0°)$	510
$A^{00}(B_{\theta\alpha})$	1.4246	V^{α}	109

[a]ZPVE = 280.590 cm^{-1}.

determined at the MP2 level of theory within the harmonic approximation. Previous studies show the relevance of this correction for obtaining reliable results.[46] The kinetic parameters, the pseudopotential and the vibrational correction of the potential energy surface, are supplied as the supplementary material. The V′ pseudopotential is very small and almost negligible.

The energies were fitted to symmetry adapted Fourier series type

$$V(\theta,\alpha) = A^{00} + \sum_{mn} A_{cc}^{nm}(\cos 3m\theta\ \cos n\alpha) + \sum_{mn} A_{ss}^{nm}(\sin 3m\theta\ \sin n\alpha). \quad (6)$$

The terms V′ and B_{ij} of the two dimensional Hamiltonian are expressed with analytical series formally identical to Eq. (6). The parameters of the final effective potential energy surface and the independent coefficients corresponding to the kinetic energy parameters are given in Tables III and IV, respectively.

For the surface, the fit parameters (R^2 = 0.999999 and σ = 1.9 cm^{-1}) guarantee the correct shape of the potential. Figure 3 represents the low energy region of the two-dimensional potential energy surface (2D-PES).

The 2D-Hamiltonian was solved variationally using ENEDIM.[32] The size of the Hamiltonian matrix was reduced considering the symmetry properties. Details about the procedure and trial functions can be found in Refs. 33, 34, and 40. The final energy levels E_{VAR} are collected in Table IV. Each level splits into 3 sublevels corresponding to the three methyl torsion minima: one nondegenerate (A_1 or A_2) and the two-degenerate (E) components. Symmetry is employed for the labeling of the levels as well as the quantum numbers n_θ, n_α.

The barrier heights are also provided in Table IV. The inversion V^α barrier at α = 0° was evaluated to be 109 cm^{-1}, while the zero point vibrational energy has been obtained to be 280.590 cm^{-1} (the contribution of the wagging mode to the ZPVE is $\nu_{15}/2 \sim 164\ cm^{-1} > V^\alpha$). This means that the very low barrier has no effect on the vibrational levels. The A_i and E subcomponents of the levels in which splitting is due to the V_3 methyl torsion barrier can be classified as the levels of a molecular species whose potential energy surface shows only three minima. One-dimensional curves of Fig. 4 can help understand this problem.

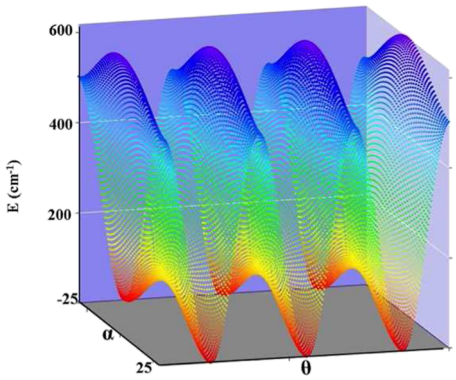

FIG. 3. The two-dimensional energy surface in the region of the minimum energy configurations.

The methyl torsion barrier was obtained to be ~500 cm^{-1} [V_3 ($\alpha = \alpha^{MIN}$) = 502 cm^{-1}; V_3 (α = 0°) = 510 cm^{-1}]. The barrier is low enough to induce non-negligible splittings. For example, the ground vibrational state splits 0.01 cm^{-1}. The lower energies belong to the excited methyl torsional states (ν_{18}) whose fundamental level has been found to lie at 168.376 cm^{-1} (A_2) and 168.013 cm^{-1} (E). $2\nu_{18}$ was computed to be 311.708 cm^{-1} (A_1) and 316.690 cm^{-1} (E). These latter levels lying below the methyl torsion barrier top shows a splitting larger than 5 cm^{-1}.

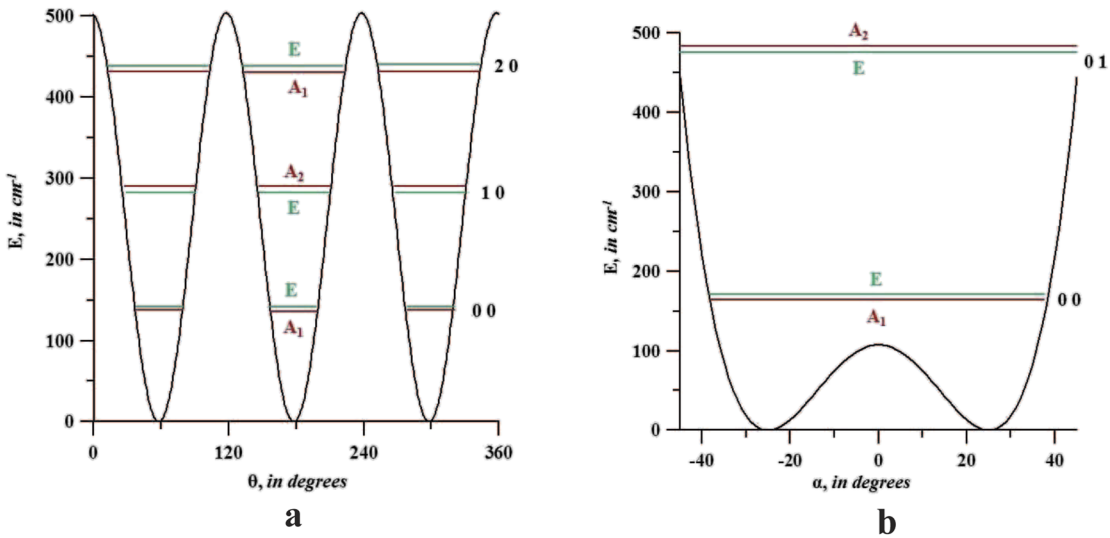

FIG. 4. Torsional energy levels located in the one-dimensional cuts of the potential energy surface as a function of (a) the θ methyl torsional coordinate, $\alpha = \alpha^{MIN}$, and (b) the α inversion coordinate, $\theta = \theta^{MIN}$.

For the methyl torsion, there is a reasonable agreement between the results obtained using the variational procedure and those derived from VPT2. However, as explained in the section titled Infrared spectrum, very relevant inconsistencies are obtained for the levels assigned to the CH_2 wagging mode where the anharmonic contributions derived from VPT2 are entirely unfounded. The fundamental ν_{15} has been determined to be 328.557 cm^{-1} (A_2) and 328.505 cm^{-1} (E) using the variational procedure far away from the result of 190.9 cm^{-1} obtained with VPT2. According to VPT2, the molecule is treated as a semirigid species with a single C_1 minimum of very low stability given the size of the V^{α} barrier.

The results of the variational calculations correspond to a molecular structure with a potential energy surface of three equivalent minima of C_s symmetry. The splittings of the levels are due to the methyl group torsion because the CH_2 torsion is expected to carry out negligible effects. In addition, the wagging mode has no effect because the levels lie over the inversion barrier. For further assignments of the experimental spectra, RDME must be treated as a C_s species instead of an asymmetric species. This last structure is not visible in experiments because measurements are not possible below the ZPVE.

CONCLUSIONS

In this paper, we provide structural and rovibrational parameters for a methoxymethyl radical, an undetected but relevant astrophysical molecule that has not been previously characterized in a laboratory. The present work aims to help further experimental studies and astrophysical observations.

The ground electronic state of double spin-multiplicity (X^2A) appears "clean" from nonadiabatic effects. At the MRCI level of theory, the first excited electronic state, a doublet state, was found to lie at 3.95 eV. The minimum energy geometry is an asymmetric structure whose rotational constants have been predicted to be A_0 = 46 718.67 MHz, B_0 = 10 748.42 MHz, and C_0 = 9272.51 MHz. The dipole moment was determined to be 1.432D (μ_A = 0.695D, μ_B = 1.215D, μ_C = 0.302D).

Three internal motions, CH_2 wagging, and the CH_2 and the methyl torsions, can intertransform the 12 minima of the potential energy surface. The interconversion barriers are predicted to be V^{α} = 109 cm^{-1}, V^{CH_2} ~ 2000 cm^{-1}, and V_3 ($\alpha = \alpha^{MIN}$) = 502 cm^{-1}. Using VPT2, four anharmonic vibrational fundamentals are found below 500 cm^{-1}: ν_{15}, ν_{16}, ν_{17}, and ν_{18}. They can be assigned to the CH_2 wagging, COC bending, CH_2 torsion, and the methyl torsion, respectively. Since the splittings due to the CH_2 torsion are negligible, the motion can be treated as a CH_2 twist. By taking into consideration the results of the test of resonances and the *ab initio* barrier heights, a two-dimensional model depending on the methyl torsion and the CH_2 wagging can be suitable. The levels computed variationally split into 3 sublevels corresponding to the three methyl torsion minima: one nondegenerate (A_1 or A_2) and the two-degenerate (E) components, the band structure that corresponds to a surface with only three minima because the top of the inversion V^{α} barrier at $\alpha = 0°$ (109 cm^{-1}) stands below the zero point vibrational energy. The C_1 minimum energy structure cannot be observed in experiments where RDME appears as a species of C_s symmetry because it stands below the zero point vibrational energy region inaccessible for experiments.

SUPPLEMENTARY MATERIAL

The predicted Fermi displacements, the Fermi resonance parameters, the kinetic parameters, the pseudopotential, and the vibrational corrections of the two-dimensional Hamiltonian are provided as the supplementary material.

ACKNOWLEDGMENTS

This research was supported by the FIS2016-76418-P project of the "Ministerio de Ciencia, Innovación y Universidades" of Spain and the CSIC i-coop 2018 programme No COOPB20364. The authors acknowledge the COST Actions CM1401 "Our Astrochemical History" and CM1405 "MOLIM." The calculations have been performed in the CESGA and CTI-CSIC computer centers. M.C. also acknowledges the financial support from the Consejería de Conocimiento, Investigación y Universidad, Junta de Andalucía, and European Regional Development Fund (ERDF), ref. SOMM17/6105/UGR.

REFERENCES

[1] N. Balucani, C. Ceccarelli, and V. Taquet, Mon. Not. R. Astron. Soc.: Lett. **449**, L16 (2015).
[2] R. J. Shannon, R. L. Caravan, M. A. Blitz, and D. E. Heard, Phys. Chem. Chem. Phys. **16**, 3466 (2014).
[3] E. Herbst, Int. Rev. Phys. Chem. **36**, 287 (2017).
[4] S. L. Fischer, F. L. Dryer, and H. J. Curran, Int. J. Chem. Kinet. **32**, 713 (2000).
[5] H. J. Curran, S. L. Fischer, and F. L. Dryer, Int. J. Chem. Kinet. **32**, 741 (2000).
[6] C. M. Rosado-Reyes, J. S. Francisco, J. J. Szente, M. M. Maricq, and L. F. Østergaard, J. Phys. Chem. A **109**, 10940 (2005).
[7] M. M. Maricq, J. J. Szente, and J. D. Hybl, J. Phys. Chem. A **101**, 5155 (1997).
[8] J. J. Nash and J. S. Francisco, J. Phys. Chem. A **102**, 236 (1998).
[9] D. A. Good and J. S. Francisco, J. Phys. Chem. A **104**, 1171 (2000).
[10] A. Bottoni, P. D. Casa, and G. Poggi, J. Mol. Struct.: THEOCHEM **542**, 123 (2001).
[11] J. Y. Liu, Z. S. Li, J. Y. Wu, Z. G. Wei, G. Zhang, and C. C. Sun, J. Chem. Phys. **119**, 7214 (2003).
[12] Q. S. Li, Y. Zhang, and S. Zhang, J. Phys. Chem. A **108**, 2014 (2004).
[13] X. Song, H. Hou, and B. Wang, Phys. Chem. Chem. Phys. **7**, 3980 (2005).
[14] A. M. El-Nahas, T. Uchimaru, M. Sugie, K. Tokuhashi, and A. Sekiya, J. Mol. Struct.: THEOCHEM **722**, 9 (2005).
[15] H. Dong, Y. Ding, and C. Sun, J. Chem. Phys. **122**, 204321 (2005).
[16] A. J. Eskola, S. A. Carr, M. A. Blitz, M. J. Pilling, and P. W. Seakins, Chem. Phys. Lett. **487**, 45 (2010).
[17] A. J. Eskola, S. A. Carr, R. J. Shannon, B. Wang, M. A. Blitz, M. J. Pilling, P. W. Seakins, and S. H. Robertson, J. Phys. Chem. A **118**, 6773 (2014).
[18] Y. Guan, Y. Li, L. Zhao, H. Ma, and J. Song, Comput. Theor. Chem. **1096**, 7 (2016).
[19] S. Langer, E. Ljungström, T. Ellermann, O. J. Nielsen, and J. Sehested, J. Chem. Phys. Lett. **240**, 53 (1995).
[20] R. Liu, M. Maricq, Y. Li, and J. S. Francisco, J. Chem. Phys. **110**, 4410 (1999).
[21] Y. Gong and L. Andrews, J. Phys. Chem. A **115**, 3029 (2011).
[22] G. Knizia, T. B. Adler, and H.-J. Werner, J. Chem. Phys. **130**, 054104 (2009).
[23] H.-J. Werner, T. B. Adler, and F. R. Manby, J. Chem. Phys. **126**, 164102 (2007).
[24] H.-J. Werner, P. J. Knowles, G. Knizia, F. R. Manby, M. Schütz, P. Celani, T. Korona, R. Lindh, A. Mitrushenkov, G. Rauhut, K. R. Shamasundar, T. B. Adler, R. D. Amos, A. Bernhardsson, A. Berning, D. L. Cooper, M. J. O. Deegan, A. J. Dobbyn, F. Eckert, E. Goll, C. Hampel, A. Hesselmann, G. Hetzer, T. Hrenar, G. Jansen, C. Köppl, Y. Liu, A. W. Lloyd, R. A. Mata, A. J. May, S. J. McNicholas, W. Meyer, M. E. Mura, A. Nicklass, D. P. O'Neill, P. Palmieri, D. Peng, K. Pflüger, R. Pitzer, M. Reiher, T. Shiozaki, H. Stoll, A. J. Stone, R. Tarroni, T. Thorsteinsson,

and M. Wang, MOLPRO, version 2010.1, a package of *ab initio* programs, 2010, see http://www.molpro.net.
[25]M. J. Frisch, G. W. Trucks, H. B. Schlegel, G. E. Scuseria, M. A. Robb, J. R. Cheeseman, G. Scalmani, V. Barone, B. Mennucci, G. A. Petersson, H. Nakatsuji, M. Caricato, X. Li, H. P. Hratchian, A. F. Izmaylov, J. Bloino, G. Zheng, J. L. Sonnenberg, M. Hada, M. Ehara, K. Toyota, R. Fukuda, J. Hasegawa, M. Ishida, T. Nakajima, Y. Honda, O. Kitao, H. Nakai, T. Vreven, J. A. Montgomery, Jr., J. E. Peralta, F. Ogliaro, M. Bearpark, J. J. Heyd, E. Brothers, K. N. Kudin, V. N. Staroverov, R. Kobayashi, J. Normand, K. Raghavachari, A. Rendell, J. C. Burant, S. S. Iyengar, J. Tomasi, M. Cossi, N. Rega, J. M. Millam, M. Klene, J. E. Knox, J. B. Cross, V. Bakken, C. Adamo, J. Jaramillo, R. Gomperts, R. E. Stratmann, O. Yazyev, A. J. Austin, R. Cammi, C. Pomelli, J. W. Ochterski, R. L. Martin, K. Morokuma, V. G. Zakrzewski, G. A. Voth, P. Salvador, J. J. Dannenberg, S. Dapprich, A. D. Daniels, Ö. Farkas, J. B. Foresman, J. V. Ortiz, J. Cioslowski, and D. J. Fox, GAUSSIAN'09, Revision A.02, Gaussian, Inc., Wallingford CT, 2009.
[26]V. Barone, J. Chem. Phys. **122**, 014108 (2005).
[27]R. A. Kendall, T. H. Dunning, Jr., and R. J. Harrison, J. Chem. Phys. **96**, 6796 (1992).
[28]P. J. Knowles and H.-J. Werner, Chem. Phys. Lett. **115**, 259 (1985).
[29]H.-J. Werner and P. J. Knowles, J. Chem. Phys. **82**, 5053 (1985).
[30]P. J. Knowles and H.-J. Werner, Chem. Phys. Lett. **145**, 514 (1988).
[31]H.-J. Werner and P. J. Knowles, J. Chem. Phys. **89**, 5803 (1988).
[32]M. L. Senent, "ENEDIM, A variational code for non-rigid molecules," 2001, available at http://tct1.iem.csic.es/PROGRAMAS.htm.
[33]M. L. Senent, Chem. Phys. Lett. **296**, 299 (1998).
[34]M. L. Senent, J. Mol. Spectrosc. **191**, 265 (1998).
[35]Y. G. Smeyers, M. Villa, and M. L. Senent, J. Mol. Spectrosc. **117**, 66 (1996).
[36]M. L. Senent, J. Mol. Spectrosc. **343**, 28 (2018).
[37]M. Villa, M. L. Senent, R. Domínguez-Gómez, O. Álvarez-Bajo, and M. Carvajal, J. Phys. Chem. A **115**, 13573 (2011).
[38]J. M. Fernández, G. Tejeda, M. Carvajal, and M. L. Senent, Astrophys. J., Suppl. Ser. **241**, 13 (2019).
[39]P. R. Bunker and P. Jensen, *Molecular Symmetry and Spectroscopy* (NRC Research Press, Ottawa, 1989).
[40]M. L. Senent, Y. G. Smeyers, R. Dominguez-Gómez, and M. Villa, J. Chem. Phys. **112**, 5809 (2000).
[41]M. R. Aliev and J. K. G. Watson, in *Molecular Spectroscopy: Modern Research*, edited by K. N. Rao (Academic Press, New York, 1985), Vol. 3, p. 1.
[42]R. A. Motiyenko, L. Margulès, M. L. Senent, and J. C. Guillemin, J. Phys. Chem. A **122**, 3163 (2018).
[43]R. Boussesi, M. L. Senent, and N. Jaïdane, J. Chem. Phys. **144**, 164110 (2016).
[44]M. L. Senent, S. Dalbouha, A. Cuisset, and D. Sadovskii, J. Phys. Chem. **119**, 9644 (2015).
[45]I. M. Mills, in *Molecular Spectroscopy: Modern Research*, edited by K. N. Rao and C. W. Mathews (Academic Press, New York, 1972).
[46]A. G. Császár, V. Szalay, and M. L. Senent, J. Chem. Phys. **120**, 1203 (2004).